Cooperativity between Cell Contractility and Adhesion

Igor L. Novak,[1] Boris M. Slepchenko,[1] Alex Mogilner,[2] and Leslie M. Loew[1]
[1]Department of Cell Biology, University of Connecticut Health Center, Farmington, Connecticut 06030, USA
[2]Department of Mathematics, University of California, Davis, California 95616 , USA
(Received 7 July 2004; published 23 December 2004)

In living cells, the cytoskeleton connects to the extracellular environment through focal adhesions, multimolecular structures that can sense applied force. A model is presented that for the first time explains why the focal adhesions tend to high-curvature regions at the cell periphery. It is based on experimental evidence for positive feedback between adhesion formation and assembly of actomyosin bundles (stress fibers). The model predicts that the focal adhesions propagate by treadmilling with a velocity proportional to the integrin diffusion coefficient.

DOI: 10.1103/PhysRevLett.93.268109 PACS numbers: 87.16.Ka, 05.45.–a, 87.16.Ac

Living cells actively change shape and move by converting chemical energy into mechanical forces. The cytoskeleton, a complex network of polymers, plays an important role in these processes. The key cytoskeletal structures involved in active force generation are stress fibers, needle-shaped bundles of actin filaments interacting with myosin motor proteins [1]. Stress fibers are connected to the cell membrane by anchoring at complex micron-size multimolecular structures known as focal adhesions [1], through which forces are transmitted to surrounding tissues. Although the detailed mechanism of stress fiber assembly remains uncertain, current observations point to two major steps: establishment of focal adhesion sites and association of actin and myosin into contractile bundles, each connecting two such sites [2,3].

Focal adhesions not only provide the physical link between the cytoskeleton and the extracellular matrix (ECM) but also serve as a cell's tactile device probing the rigidity of the external environment [4–7]. Although the nature of mechanical sensing by focal adhesion is not fully understood, several possible mechanisms have been proposed [8] and a growing body of evidence suggests that the traction forces developed at the contact sites increase the rate of assembly of focal adhesions [9–11]. In particular, the traction generated at a ''mature,'' stationary focal adhesion was found to be proportional to its surface area.

Recent experimental discoveries point to another intriguing feature of stationary cells: most of them tend to organize long stress fibers, with large focal adhesions concentrating at the cell periphery in high-curvature regions [12–14]. A number of important questions arise from these observations. Could an adhesion/stress fiber interaction lead to this self-organizing behavior? Why is the homogeneous distribution of adhesions disfavored? Why do adhesions tend toward the cell periphery? What determines the time scale of adhesion redistribution? In this Letter we introduce a model that answers these questions and provides a quantitative framework for the interpretation of experimental observations.

Consider a stationary cell with a given geometry Ω (Fig. 1). For simplicity, we will follow the dynamics of only the key surface receptors mediating adhesion assembly, integrins, while the detailed kinetics of other adhesion proteins is omitted. Because the numbers of stress fibers and integrins are large enough we describe them in terms of their densities and concentrations.

Adhesions are characterized by the local density of the integrins bound to ECM, $\rho(\mathbf{X}, t)$ $[\mu\mathrm{m}^{-2}]$. According to experiments, this density increases in proportion to the magnitude of the force (per unit area), $|\mathbf{F}(\mathbf{X}, t)|$, generated at the adhesion site by stress fibers [9], and the local concentration of unbound integrins, $\rho^*(\mathbf{X}, t)$ $[\mu\mathrm{m}^{-2}]$. Also, adhesions can disassemble with a constant rate k_{-1}. Unbound integrins are free to diffuse in the cell membrane with the diffusion coefficient D. We assume random isotropic nucleation of stress fibers at the adhesion sites, with the rate proportional to the adhesion size. Therefore, the force generated by a stress fiber grows in proportion to the number of integrins in each of the adhesions it connects. The corresponding rate constant, $k_2 f_0$ (f_0 is the force generated by a ''unit'' actomyosin filament) is assumed, for simplicity, to be independent of distance between the

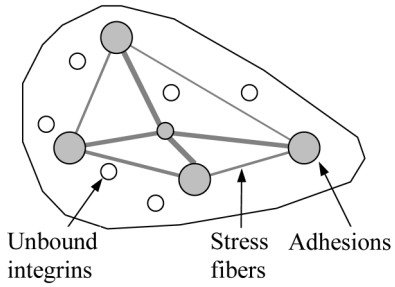

FIG. 1. Schematic representation of adhesion-stress fiber interaction (top view of a thin cell lying on a flat 2D substratum). Tension generated along the stress fibers causes focal adhesions to stabilize and grow. Unbound integrins freely diffuse in the 2D cell membrane. New stress fibers, are nucleated at focal adhesions.

adhesions. This is in line with the fact that long and short stress fibers are observed in roughly equal proportion in nonmoving cells. Bundles can also disassemble with a constant rate k_{-2}. Overall, the model is described as follows:

$$\frac{\partial \rho}{\partial t} = [k_0 + k_1|\mathbf{F}(\mathbf{X}, t)|]\rho^* - k_{-1}\rho,$$
$$\frac{\partial \rho^*}{\partial t} = -[k_0 + k_1|\mathbf{F}(\mathbf{X}, t)|]\rho^* + k_{-1}\rho + D\nabla^2\rho^*, \quad (1)$$
$$\frac{\partial \mathbf{F}}{\partial t} = k_2 f_0 \rho \int_\Omega \rho(\mathbf{X}', t)\frac{\mathbf{X}' - \mathbf{X}}{|\mathbf{X}' - \mathbf{X}|}d^2X - k_{-2}\mathbf{F}.$$

The first two equations represent mass conservation of the bound and free integrins; k_0 is the rate of force-independent assembly of adhesions. Typically, $k_0 \ll k_{-1}$, which follows from the observation that cells form only small adhesions if the generation of force is inhibited [9]. The third equation, a kinetic law for the force $\mathbf{F}(\mathbf{X}, t)$, is obtained by integrating forces produced by all stress fibers originating at point $\mathbf{X}$ [15]. In the present form, the model includes eight parameters: k_0, k_1, k_{-1}, k_2, k_{-2}, f_0, D, and the average concentration of the bound and free integrins $\bar{\rho}$ (through the zero-flux boundary condition for free integrins). Nondimensionalization reduces this number to four. Define the dimensionless density of bound integrins $c = \rho/\bar{\rho}$, density of free integrins $c^* = \rho^*/\bar{\rho}$, force $\mathbf{f} = \mathbf{F}k_{-2}/|\Omega|k_2 f_0\bar{\rho}^2$, space variable $\mathbf{x} = \mathbf{X}/\sqrt{|\Omega|}$: $\Omega \to \tilde{\Omega} \subset R^2$, and time $\tau = tk_{-2}$. Equations (1) then take the form

$$\frac{1}{\alpha}\frac{\partial c}{\partial \tau} = (\alpha_0 + |\mathbf{f}|)c^* - \beta c,$$
$$\frac{1}{\alpha}\frac{\partial c^*}{\partial \tau} = -(\alpha_0 + |\mathbf{f}|)c^* + \beta c + \frac{\tilde{D}}{\alpha}\nabla^2 c^*, \quad (2)$$
$$\frac{\partial \mathbf{f}}{\partial \tau} = c\int_{\tilde{\Omega}} c(\mathbf{x}', \tau)\frac{\mathbf{x}' - \mathbf{x}}{|\mathbf{x}' - \mathbf{x}|}d^2x - \mathbf{f},$$

where $\beta = k_{-1}k_{-2}/k_1k_2f_0\bar{\rho}^2|\Omega|$, $\alpha_0 = \beta k_0/k_{-1}$, $\alpha = k_{-1}/\beta k_{-2}$, and $\tilde{D} = D/|\Omega|k_{-2}$ are the nondimensional parameters of the model. The typical cell size is $\sim 30\ \mu$m, and time scales are as follows: seconds for binding/unbinding of integrins from adhesions [9], minutes for assembly/disassembly of stress fibers [2], and $D \sim 10^{-4}$–$10^{-1}\ \mu$m^2/sec [16]. This yields the following ranges for nondimensional parameters: $\alpha_0 \sim 10^{-3} - 10^{-1}$, $\beta \sim 10^{-2} - 1$, $\alpha \sim 10^4 - 10^2$, $\tilde{D} \sim 10^{-5} - 10^{-2}$.

The analysis of the steady state is particularly simple and instructive in the case with $D = \infty$ and large k_2 and k_{-2} so that the stress fibers are in instantaneous equilibrium with the adhesion density field $c(\mathbf{x})$. In this case, the redistribution of focal adhesions is driven by their interaction with the self-induced force field $\mathbf{E} = (\mathbf{f}/c) = \int_{\tilde{\Omega}} c(\mathbf{x}', \tau)[(\mathbf{x}' - \mathbf{x})/|\mathbf{x}' - \mathbf{x}|]d^2x$. In dimensional units $\mathbf{E}$ is of the order of f_0, and represents the force acting on a unit integrin at point $\mathbf{x}$. One then can show that for any distribution $c(\mathbf{x})$, $|\mathbf{E}|$ increases from a unique point inside the cell where $|\mathbf{E}| = 0$ to the boundary $\partial\tilde{\Omega}'$ [17]. Because c^* is spatially uniform in this case, it follows from the first of Eqs. (2) that the local concentration of adhesions always grows faster at the periphery and eventually adhesions will accumulate in an infinitely small boundary layer, just as free charges in a conductor are pushed out to the surface by their self-induced electric field [18]. In the further steady-state analysis, because the adhesion density at the boundary rises to infinity, it is convenient to switch from concentrations and densities to the "mass-type" variables M, such that $c = dM/d\mathbf{x}$. "Masses" are bounded, and therefore attain steady-state values if they exist.

We now turn to a rigorous analysis of a general 1D case ($D < \infty$), $x \in \tilde{\Omega} = [0, 1]$. To find the steady state, we introduce the monotonic variable $M(x) = \frac{1}{2}\int_0^1 c(x')\mathrm{sgn}(x - x')dx'$, and make use of spatial uniformity of stationary c^*. Convolving the first and the third of Eqs. (2) with $\mathrm{sgn}(x)$ yields the following steady-state equation:

$$\left(x - \frac{1}{2}\right)\alpha_0 + M|M| = \frac{\beta M}{1 + 2M(0)}, \quad (3)$$

where $M(0) = -\frac{1}{2}\int_0^1 c\,dx = -M(1)$ [19]. Depending on α_0 and β, Eq. (3) may have up to three different solutions corresponding to different roots of the cubic polynomial, $M^3(0) + \frac{1}{2}M^2(0) + [(\beta + \alpha_0)/2]M(0) + \frac{\alpha_0}{4} = 0$.

There are two qualitatively different patterns of adhesion distribution at steady state: $M(x)$ may be either a continuous differentiable function (the inactive state) or may have two discontinuities at $x = 0$ and $x = 1$ (the active state) [20]. Stability of these solutions can be established analytically for the case $0 \le \alpha_0 \ll \beta$. The results that turned out to be independent of $\tilde{D}$ and α are shown for $\alpha_0 = 0$ in Fig. 2(a). In the inactive state, "weak" adhesions are distributed over the whole cell surface, whereas in the active state, along with distributed small adhesions, the cell has two large adhesions located at the periphery points $x = 0$ and $x = 1$ [Fig. 2(b)]. In the region of bistability, $\beta < 1/8$, in the limit $\alpha_0 \to 0$, $\tilde{D} \to \infty$, the domain of attraction of the active state is determined by a critical initial amount of bound integrins. This threshold drops as β decreases. Numerical experiments with realistic values of $\tilde{D}$ and α_0 show similar trends. Thus, the system is most likely to be active when β is small (integrins firmly associate with ECM), which is typical for the wild-type cells [Fig. 4(b)]. One way to increase β is by impeding fiber formation. Indeed, continuous adhesion distributions observed in mutants with the inhibited assembly of stress fibers [21] is consistent with the inactive state of the model.

Dynamics of the 1D system have been studied numerically. Simulation results in Figs. 3(a)–3(c) illustrate the specific way in which adhesions, initially concentrated in the center of a 1D fragment, move to its end points. This movement occurs in a treadmilling manner. At the initial stage, the density peak splits into two because of the zero net force at its midpoint. As disassembly of adhesions in the space between the peaks continues, the released integrins get recruited at the fronts almost immediately, because of fast binding and slow diffusion. A steep gradient of free integrins (see Fig. 3), which is due to substantial difference

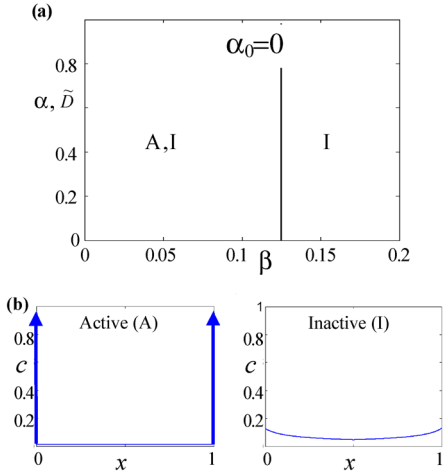

FIG. 2 (color online). (a) Steady-state phase diagram in 1D ($\alpha_0 = 0$). At $\beta < 1/8$, there are two stable states: active (A) and inactive (I); otherwise, only the inactive state exists. (b) Patterns of steady-state adhesion distribution: discontinuous distribution with large adhesions at the end points in the active state (left), and continuous low-density distribution in the inactive state (right).

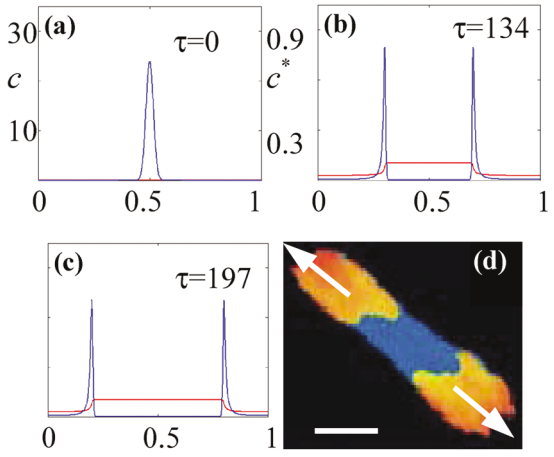

FIG. 3 (color). (a)–(c) Propagation of adhesions to the ends of a 1D fragment. Numerical solution of 1D Eqs. (2) with $\alpha_0 = 0.01$, $\alpha = 100$, $\beta = 0.025$, $\tilde{D} = 0.01$. Densities of bound (blue line) and free (red line) integrins are plotted along the y axis. Initially, there are no stress fibers, and adhesions are concentrated in the center of the fragment. (d) Adhesion doublet formed from an isolated cluster of bound integrins: fluorescent adhesion protein and stress fibers are shown in red and blue, respectively. Arrows indicate the direction of the doublet expansion. Bar $\approx$ 2 μm (adapted from [23]).

in the rates of binding at the rear and the front of the peaks, leads to diffusion of free integrins ahead of the front, and therefore drives treadmilling of adhesions towards the periphery. The dynamic redistribution of adhesions to the cell periphery was observed experimentally [Fig. 2(a) in [21], Fig. 1(a) in [22]]. Moreover, isolated aggregates of bound integrins, mimicked by the initial conditions in Fig. 3(a), were indeed shown to transform into expanding circles or quasi-1D "doublets," as stress fibers were being formed [Fig. 3(d)] [23].

Of particular interest is an estimate of the time necessary for adhesions to move to the cell periphery. This estimate can be obtained by approximating a solution of Eqs. (2) as traveling waves propagating in opposite directions. The wave velocity, v, can then be obtained by direct substitution of a traveling wave solution into Eqs. (2). In the case of slow diffusion, $\sqrt{\tilde{D}}c^*_{\rm int}/\beta\sqrt{\alpha\beta} \ll 1$ (also, $\alpha_0 \ll \beta$), this yields $v \propto \tilde{D}c^{*2}_{\rm int}/\beta$ ($c^*_{\rm int}$ is the concentration of free integrins in the interior between the peaks and is of the order of β). As the peaks approach the boundary, they either accumulate at the end points or disperse, depending on the parameter values (see Fig. 2).

Note that in the diffusion-limited case, v depends on $\tilde{D}$ in our model as $v \propto \tilde{D}/\lambda$, $\lambda = \beta/c^{*2}_{\rm int}$, in contrast with $v \propto \sqrt{\tilde{D}}$, commonly found for waves in reaction-diffusion systems. Our situation is somewhat analogous to the "fire-diffuse-fire" type of intracellular calcium waves [24], where diffusive Ca ion is released at discrete sites separated by a distance l when local Ca concentration exceeds a certain threshold. In this case, if l is large, Ca diffusion ($D_{\rm Ca}$ is a diffusion coefficient) is the most time-consuming step, and $v \propto D_{\rm Ca}/l$. In our case, diffusion is also a limiting step and "firing" is the release of integrins from the rear of the peak. In order to trigger this event, free integrins should diffuse from the rear to the front in the amount exceeding a certain threshold. This threshold amount must be comparable with that in the peak, as these integrins balance the force in the rear after they get bound. This means that the "threshold diffusion length" δ is of the order of the peak width. Because diffusion on this length occurs in the presence of fast and strong binding, the effective diffusion coefficient is $D_{\rm eff} = \tilde{D}\delta/\lambda$ where $\lambda = \beta/c^{*2}_{\rm int}$ is the length that would be occupied by the threshold amount of integrins in the free form. Finally, as diffusion is the time-limiting process, $v \propto D_{\rm eff}/\delta = \tilde{D}/\lambda$.

The basic property of the 1D model is preserved in a realistic 2D case: large focal adhesions tend to relocate to the cell periphery [Fig. 4(c)]. Qualitatively, this behavior can be explained based on the following observations. The net force acting on adhesions in the central region of the cell is small because the stress fibers growing in different directions compensate each other's actions. At the periphery, on the other hand, fibers are directed into the interior of the cell and the net force is relatively large. Therefore, at the periphery adhesions will assemble more rapidly than in the central region. This translocation will alter the orientation of the stress fibers with most of them growing from the periphery. Such a positive feedback will ultimately result in accumulation of adhesions at the boundary.

The numerical solution of Eqs. (2) on a square [Fig. 4(c)] can be directly compared to the experimental data on cells cultured on square islands of substratum [Fig. 4(b)] [12]. The main trend observed in the experiment appears to be in close agreement with the theory: focal adhesions relocate to the cell periphery and concentrate at the corners, i.e., at the regions with the highest boundary curvature (see also

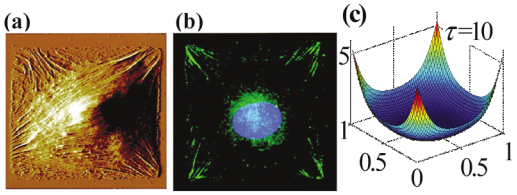

FIG. 4 (color). Experiment and simulation of the pattern of cell adhesion on a square substrate. (a) Cell landscape imaged with the atomic force microscope. Diagonal lines originating at the corners are stress fibers. (b) Fluorescent focal adhesion protein, vinculin (green) [12]. (c) Adhesion density as a function of position on a square cell membrane. Numerical solution of Eqs. (2) on a square at time $\tau = 10$, with $\alpha_0 = 0.001$, $\alpha = 100$, $\beta = 0.1$, $\tilde{D} = \infty$. Initially, there were no stress fibers, and adhesions were concentrated in the center of the square.

experiments by Brock *et al* [13] for a variety of substratum island shapes).

Interestingly, the fact that the steady-state adhesion distribution at the cell boundary follows qualitatively the curvature of the boundary (Fig. 5) is reminiscent of the electrostatic distribution of charges over the surface of a conductor [18], though in our case, as follows from Eqs. (2) with $\alpha_0 \ll \beta$, this distribution is approximately governed by the integral equation $|\mathbf{E}| = \text{const}$, $\mathbf{E} = \int_{\tilde{\Omega}} c(\mathbf{x}')[(\mathbf{x}' - \mathbf{x})/|\mathbf{x}' - \mathbf{x}|]d^2x$. This property of the adhesion distribution in our model can be qualitatively understood based on the observation that at the high-curvature regions, the sum of unit vectors directed along stress fibers is amplified. The required net force field can therefore be achieved with lower than average concentrations distributed outside the high-curvature region thus leading to higher than average concentration at the locations with high-curvature.

In conclusion, long stress fibers and a highly nonuniform distribution of focal adhesions are explained by the positive feedback between cell contractility and adhesion. Although the assembly/disassembly processes are relatively fast, the redistribution of adhesions occurs on the slow time scale determined by diffusion of free integrins. The model predicts that this slow time scale is in hour range, which is in agreement with observations [23].

Note that our theory directly applies to stationary cells. In moving cells, the situation is more complex: enzymatic activities regulate the adhesion dynamics at the cell leading edge differently from that in the cell interior [25]. However, in moving cells, large adhesions also tend to translocate to the cell edge [26]. The model, therefore, captures general features of adhesion/contractility dynamics and can be extended to account for more complex processes in moving cells.

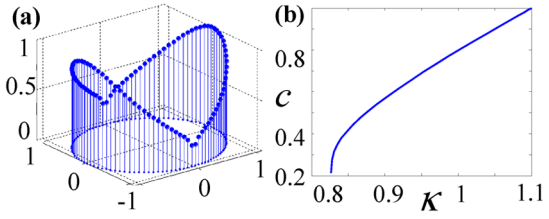

FIG. 5 (color online). (a) Steady-state distribution of adhesions along the boundary of an ellipsoidal cell with the eccentricity $e = 0.42$. Adhesion density is plotted in arbitrary units ($\alpha_0 = 0$). (b) Adhesion density c as a function of curvature k. (Note, that this dependence becomes significantly nonlinear at the points with sufficiently low curvature.)

We thank B. Geiger, A. R. Horwitz, I. Moraru, J. E. Pearson, and M. A. Schwartz for helpful discussions and suggestions. This work was supported by NIH Grants No. U54 GM64346 and No. P41 RR13186.

[1] B. Alberts *et al.*, *Molecular Biology of the Cell* (Garland Publishers, New York, 1994), 3rd ed.
[2] Y. L. Wang, J. Cell Biol. **99**, 1478 (1984).
[3] K. Katoh *et al.*, Mol. Biol. Cell **9**, 1919 (1998).
[4] C. G. Galbraith and M. P. Sheetz, Curr. Opin. Cell Biol. **10**, 566 (1998).
[5] R. J. Pelham and Y. Wang, Proc. Natl. Acad. Sci. U.S.A. **94**, 13661 (1997).
[6] B. Geiger and A. Bershadsky, Cell **110**, 139 (2002).
[7] D. E. Ingber, Proc. Natl. Acad. Sci. U.S.A. **100**, 1472 (2003).
[8] B. Geiger and A. Bershadsky, Curr. Opin. Cell Biol **13**, 584 (2001).
[9] N. Q. Balaban *et al.*, Nat. Cell Biol. **3**, 466 (2001).
[10] J. L. Tan *et al.*, Proc. Natl. Acad. Sci. U.S.A. **100**, 1484 (2003).
[11] W. M. Petroll, L. Ma, and J. V. Jester, J. Cell Sci. **116**, 1481 (2003).
[12] K. K. Parker *et al.*, FASEB J. **16**, 1195 (2002).
[13] A. Brock *et al.*, Langmuir **19**, 1611 (2003).
[14] C. S. Chen *et al.*, Biochem. Biophys. Res. Commun. **307**, 355 (2003).
[15] In Eq. (1), fibers are described as straight lines. However, if there is an obstacle between the adhesions, the fiber, which is always under contractile tension, will connect them along the shortest path in Ω. This generalization does not affect the results.
[16] A. F. Horwitz (private communication).
[17] $\mathbf{E} = \nabla\varphi$, where $\varphi = \int_{\tilde{\Omega}} c(\mathbf{x}')|\mathbf{x}' - \mathbf{x}|d^2x$ is a convex function with a unique local minimum.
[18] L. D. Landau, E. M. Lifshitz and L. P. Pitaevskii, *Electrodynamics of Continuous Media* (Pergamon, Oxford, 1984), 2nd ed.
[19] Note that the solution of Eq. (3) is an odd function with respect to $x = 1/2$.
[20] In the active state $\lim_{x\to 0} M(x) \neq M(0)$, yielding $c(0) = M'(0) = \infty$.
[21] C. Ballestrem *et al.*, J. Cell Biol. **155**, 1319 (2001).
[22] D. J. Webb *et al.*, Nat. Cell Biol. **6**, 154 (2004).
[23] B. Zimerman, T. Volberg, and B. Geiger, Cell Motil. Cytoskeleton **58**, 143 (2004).
[24] S. P. Dawson, J. Keizer, and J. E. Pearson, Proc. Natl. Acad. Sci. U.S.A. **96**, 6060 (1999).
[25] J. V. Small and I. Kaverina, Curr. Opin. Cell Biol. **15**, 40 (2003).
[26] D. J. Webb, J. T. Parsons, and A. F. Horwitz, Nat. Cell Biol. **4**, 97 (2002).